

Chitosan/Biphasic Calcium Phosphate Composite Scaffold Incorporated with
Trichostatin A for Bone Regeneration



A Dissertation Submitted in Partial Fulfillment of the Requirements
for the Degree of Doctor of Philosophy in Oral Biology

Common Course

FACULTY OF DENTISTRY

Chulalongkorn University

Academic Year 2021

Copyright of Chulalongkorn University

โครงเลี้ยงเซลล์ที่ขึ้นรูปจากโคโตนาน / ไบโอฟาสติกแคลเซียมฟอสเฟตและบรรจุด้วยสารไตรโคสแตตินเอ
เพื่อใช้สำหรับกระบวนการซ่อมแซมกระดูก



วิทยานิพนธ์นี้เป็นส่วนหนึ่งของการศึกษาตามหลักสูตรปริญญาวิทยาศาสตรดุษฎีบัณฑิต
สาขาวิชาชีววิทยาช่องปาก ไม่สังกัดภาควิชา/เทียบเท่า
คณะทันตแพทยศาสตร์ จุฬาลงกรณ์มหาวิทยาลัย
ปีการศึกษา 2564
ลิขสิทธิ์ของจุฬาลงกรณ์มหาวิทยาลัย

ธีรวัฒน์ สุขไผ่ตา : โครงเลี้ยงเซลล์ที่ขึ้นรูปจากไคโตซาน / ไบพาสติกแคลเซียมฟอสเฟต และบรรจุด้วยสารไตรโคสแตตินเอ เพื่อใช้สำหรับกระบวนการซ่อมแซมกระดูก.

(Chitosan/Biphasic Calcium Phosphate Composite Scaffold Incorporated with Trichostatin A for Bone Regeneration) อ.ที่ปรึกษาหลัก : รศ. ดร.รัชณี อัมพร อร่ามเวทย์

การศึกษาวิจัยในครั้งนี้มีวัตถุประสงค์เพื่อพัฒนาโครงเลี้ยงเซลล์ที่มีไคโตซานเป็นองค์ประกอบหลัก และบรรจุด้วยสารไตรโคสแตตินเอ เพื่อใช้สำหรับกระบวนการซ่อมแซมกระดูก โครงเลี้ยงเซลล์ที่มีสัดส่วนของไบพาสติกแคลเซียมฟอสเฟต 0%, 10%, 20% และ 40% ได้รับการขึ้นรูปด้วยวิธีทำเยือกแข็ง ผลการศึกษาวิจัยพบว่าการเพิ่มขึ้นของสัดส่วนไบพาสติกแคลเซียมฟอสเฟต ช่วยปรับปรุงคุณสมบัติเชิงกล และลดอัตราการละลายตัวของโครงเลี้ยงเซลล์ได้ และคุณสมบัติโดยรวมของโครงเลี้ยงเซลล์ที่มีสัดส่วนของไบพาสติกแคลเซียมฟอสเฟต 20% มีความเหมาะสมมากที่สุดสำหรับการพัฒนา นอกจากนี้ผู้วิจัยได้ทำการศึกษาถึงความเข้มข้นที่เหมาะสมของสารไตรโคสแตตินเอ จากผลการวิจัยพบว่า โครงเลี้ยงเซลล์สามารถนำส่งสารไตรโคสแตตินเอได้ถึงสามวัน และโครงเลี้ยงเซลล์ที่บรรจุสารไตรโคสแตตินเอที่ระดับความเข้มข้น 800 นาโนโมลาร์มีความเข้ากันได้กับเซลล์มากที่สุด และยังสามารถกระตุ้นการแสดงออกของยีนที่เกี่ยวข้องกับการสร้างกระดูกในเซลล์เอ็นดอทีลียัลของมนุษย์ได้ จากการศึกษาโดยใช้รอยวิการกะโหลกศีรษะหนูเมาส์ และทำการศึกษาเปรียบเทียบกระดูกที่สร้างขึ้นใหม่โดยการถ่ายภาพรังสีไมโครคอมพิวเตอร์โทโมกราฟีและการวิเคราะห์ทางจุลกายวิภาคในสัปดาห์ที่ 6 และ 12 หลังการผ่าตัด ผลการศึกษาพบว่ากลุ่มที่ใส่โครงเลี้ยงเซลล์ชนิดที่บรรจุสารไตรโคสแตตินเอสามารถกระตุ้นการสร้างกระดูกใหม่ได้มากกว่ากลุ่มควบคุมอย่างมีนัยสำคัญ โดยที่เนื้อเยื่อกระดูกที่สร้างขึ้นใหม่มีความต่อเนื่องไปกับรอยวิการกระดูกเดิม ผลการวิจัยสรุปได้ว่าโครงเลี้ยงเซลล์ไคโตซาน/ไบพาสติกแคลเซียมฟอสเฟต ที่บรรจุสารไตรโคสแตตินเอ มีคุณสมบัติเหมาะสมสำหรับการพัฒนาเพื่อใช้ในกระบวนการวิศวกรรมเนื้อเยื่อกระดูก

สาขาวิชา ชีววิทยาช่องปาก

ลายมือชื่อนิสิต

ปีการศึกษา 2564

ลายมือชื่อ อ.ที่ปรึกษาหลัก

6176057132 : MAJOR ORAL BIOLOGY

KEYWORD: Chitosan, Biphasic calcium phosphate, Trichostatin A, Bone regeneration

Teerawat Sukpaita : Chitosan/Biphasic Calcium Phosphate Composite Scaffold Incorporated with Trichostatin A for Bone Regeneration. Advisor: Assoc. Prof. RUCHANEE AMPORNARAMVETH, Ph.D.

This study synthesized a chitosan-based scaffold incorporated with trichostatin A (TSA), an epigenetic modifier molecule, using a freeze-drying technique to achieve promising bone regeneration potential. The scaffolds with various biphasic calcium phosphate (BCP) proportions: 0%, 10%, 20%, and 40% were characterized. The addition of BCP improved the scaffolds' mechanical properties and delayed the degradation rate. From all physicochemical parameters, 20% BCP scaffold matched the appropriate bone scaffold requirements and was selected for further development. The proper concentration of TSA was also tested. Our developed scaffold released TSA and sustained them for up to 3 days. The scaffold with 800 nM of TSA showed excellent biocompatibility and induced osteoblast-related genes expression in the primary human periodontal ligament cells (hPDLs). To evaluate *in vivo* bone regeneration potential, the scaffolds were implanted in the mice calvarial defect model. The excellent bone regeneration ability of the CS/BCP/TSA scaffolds was further demonstrated in the micro-CT and histology sections compared to both negative control and commercial bone graft product. New bone formed in the CS/BCP/TSA group revealed a trabeculae-liked structure characteristic of the mature bone at both 6 and 12 weeks. The CS/BCP/TSA scaffold is an up-and-coming candidate for the bone tissue engineering scaffold.

Field of Study: Oral Biology

Student's Signature

Academic Year: 2021

Advisor's Signature

ACKNOWLEDGEMENTS

This research was supported by The Royal Golden Jubilee Ph.D. Program (PHD/0040/2561); Chulalongkorn University Laboratory Animal Center (CULAC), Animal use protocol No. 2073027; The 90th Anniversary of Chulalongkorn University Scholarship (Batch 50).

Teerawat Sukpaita



CHAPTER 1 INTRODUCTION

1.1 Background and Rationale

Recent advancements in bone tissue engineering (BTE) with 3D porous scaffolds have long been considered in bone defect repair. The development of BTE materials requires the improvement of porous bone scaffolds that have appropriate mechanical properties with suitable porosity. The incorporation of growth factor molecules that promote new bone formation is essential.

In order to develop bone substitute material with high biocompatibility and excellent osteogenic capacity. Chitosan, a copolymer derived from chitin's deacetylation, is of our interest. To enhance the mechanical properties of chitosan for bone tissue engineering applications, several studies tried to incorporate bio-ceramic into the chitosan scaffolds. One of the most exciting bio-ceramic is biphasic calcium phosphate (BCP) exhibiting good bioactivity and optimum degradation rates under physiological conditions. Due to the osteoinductive property of chitosan, the bone formation capability of chitosan composites scaffold could still be improved or fastened by incorporating appropriate biomolecules.

In the context of molecular biology, DNA molecules of mammalian cells regulate their function partly by changing their three-dimensional structure, coiling, and uncoiling, by wrapping twice around a histone octamer to make a nucleosome. The acetylation and deacetylation process of histones proteins largely affect their interaction with DNA and therefore alter the transcription of genes resided on the corresponding region of DNA. Histone acetylation, which opens up the chromatin structure, is catalyzed by histone acetyltransferase (HAT), while deacetylase, which results in a condensation of chromatin, is influenced by histone deacetylase (HDAC). Trichostatin A (TSA) is a broad-spectrum HDAC inhibitor. TSA has been reported to induce accumulation of

acetylated histone tail which renders loosening, euchromatin, structure more accessible for the transcriptional complexes and therefore turning on the transcription of genes in mammalian cells. Many previous studies have demonstrated that TSA specifically induces *in vitro* osteoblast differentiation and enhances *in vivo* bone regeneration. Therefore, TSA might be an excellent therapeutic agent for bone tissue engineering applications to incorporate into a 3D porous scaffold.

In this study, we intend to develop a chitosan biphasic calcium phosphate composite scaffold incorporated with trichostatin A (CS/BCP/TSA scaffold) and examine their mechanical and biological properties *in vitro* and *in vivo* experiments.

Research question

Can BCP incorporation improve the mechanical properties of chitosan scaffold?

Can CS/BCP/TSA scaffold enhance bone regeneration?

Research objective

1.2.1 To examine the mechanical and biological properties of CS/BCP/TSA scaffold.

1.2.2 To compare the ability of new bone formation induced by CS/BCP scaffold, CS/BCP/TSA scaffold, and commercial bone graft products in mouse calvarial defects.

Hypothesis

H0: 1. CS/BCP/TSA scaffold does not demonstrate appropriate mechanical and biological properties for bone regeneration.

2. CS/BCP/TSA scaffold does not demonstrate the ability to induce new bone formation *in vivo*.

H1: 1. CS/BCP/TSA scaffold has appropriate mechanical and biological properties for bone regeneration.

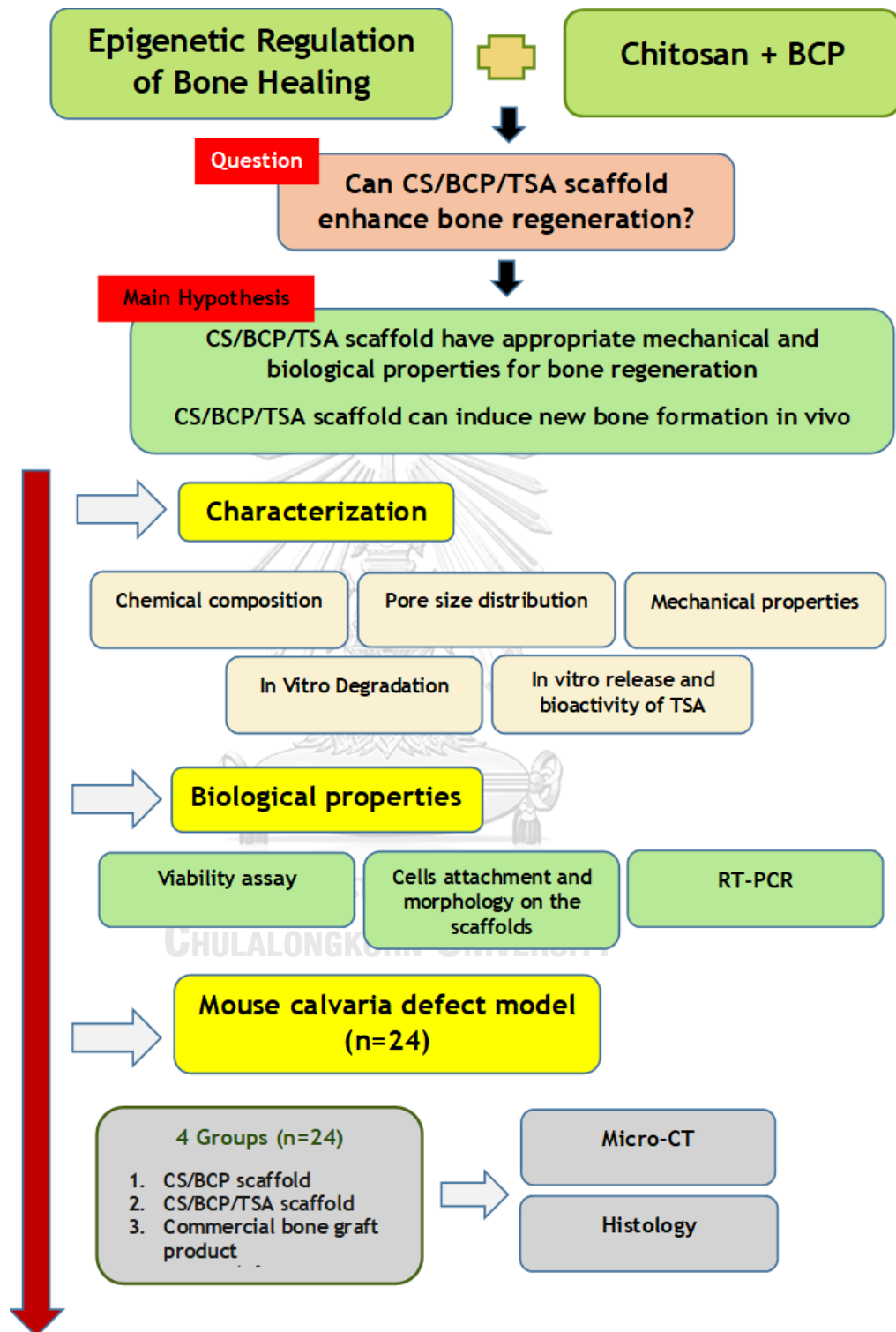
2. CS/BCP/TSA scaffold has the ability to induce new bone formation in vivo.

Expected benefits

The knowledge from this study could propose a novel alternative material for bone regeneration. The information about mechanical properties, biological properties, and the ability to enhance the bone formation of a novel CS/BCP/TSA scaffold will be clarified. The newly developed scaffold could repair and fasten the healing of damaged bone defects with promising results.



Conceptual framework



CHAPTER 2 LITERATURE REVIEW

2.1 Bone regeneration

Bone is a complex dynamic organ that structurally composes cortical and cancellous parts with remarkable regenerative properties. Despite its dynamic property, bone structure is rigid and provides multiple supporting roles for many organs. The complexity of bone architectures harmonizes altogether the living bone cells and organic and inorganic extracellular structures to allow bone tissue to perform both biological and mechanical functions (1, 2). Compact bone is the outermost compartment and accounts for 80% of the total bone mass. Besides its primary function as a core framework to support and protect other vital organs, the cortical bone compartment provide levers for movement and acts as a reservoir to store the mineral content of our body. The inner compartment of bone is referred to as the trabecular or cancellous bone. Trabecular bone, a sponge-like tissue, is composed of the lacunae and osteocytes in a lattice-like network in trabecular space. Trabecular bone contains a lot more surface area with higher metabolic activity.

Osteoblasts develop from an undifferentiated precursor of the mesenchymal origin, while osteocytes are osteoblasts that are entombed in the calcified matrix. In contrast, osteoclasts arise from blood-borne monocytes derived from distinctively different hematopoietic stem cells origin. The processes of bone remodeling require both depositions of a new bone by osteoblasts in concert with the matrix resorption capability of osteoclasts. These processes shape and reshape bones during growth and continue throughout life making bone the vital organs. Physiologic remodeling shapes a piece of bone according to its function and depending on its anatomical site

but will not immensely change bone shape due to the balance between bone resorption and bone deposition repeatedly occurring in the exact location.

Over the years, bone grafts are still considered the standard treatment for bone repair and bone augmentation. However, several limitations of conventional bone graft materials obstruct this standard treatment's utilization. Still, the quantity of donor bone available is often limited. Several adverse consequences might occur such as donor site morbidity, associated infection, chronic pain, and rapidly resorbable. Moreover, allograft and xenograft introduce the risk of disease or cross-infection (3).

Bone tissue engineering uses the principles of engineering and biology to develop biological substitutes to restore, maintain, or improve its function. Bone tissue engineering requires three components: a morphogenetic growth signal that enhances new bone formation, the bone cells that will be responded to the signal, and the suitable scaffold that can serve as the host cells and support three-dimensional bone tissue formation (4, 5).

Cell approaches in bone tissue engineering

One of the most critical components of mineralized tissue engineering is progenitor cells. Providing osteoprogenitor cells with the intrinsic potential to regenerate bone could result better. However, the availability of the cell sources that have the potential to differentiate into osteoblasts and form neo-vasculature that could be implanted into the bone defect is the main obstacle. Identification of possible candidates for cell transplantation can be explained by the finding that those cells demonstrate a capability to reconstruct osseous tissue by undergoing a progressive differentiation from undifferentiated progenitor cells to biosynthetically mature cells (5).

Scaffold

Due to the recent rapid development of novel medical technologies, novel materials are being developed. Scaffold materials for cell seeding play an essential role in bone tissue engineering. The scaffold is vital for cell homing, proliferating, and forming new osseous tissue in three dimensions. A critical consideration in selecting an ideal scaffold for bone tissue engineering (Table 1) includes, for example, biocompatibility, biodegradability, promoting cellular activities, and possessing good physical and mechanical properties (6).

Table 1 Select criteria for bone tissue engineering scaffold.

Properties of bone tissue engineering scaffold	
1.	Osteoinduction
2.	Osteoconduction
3.	Degradation rates of a scaffold according to new bone growth
4.	Appropriate mechanical and physical properties
5.	Good bony apposition
6.	Promotes osteoblast ingrowth
7.	It does not induce soft tissue growth
8.	Minimal inflammation of surrounding tissue
9.	Sterilizable without loss of properties

Table 2 Considerations for scaffold design used in bone tissue engineering. (7)

Criteria	Function
Biocompatibility	The ability of a material to perform with an appropriate host response in a specific situation without an immune response
Biodegradability	The degradation rate of the scaffold consistent with

	new bone formation
Mechanical properties	Appropriate mechanical properties to provide temporary support
Osteoinductivity	Osteoprogenitor cells can be stimulated when the presence of scaffolds
Porosity	Proper pore size to allow osteoprogenitor cells ingrowth

2.3 Types of scaffolds

There is a rapid increase in the number of novel scaffolds that have been developed for bone tissue engineering (Table 3) (7, 8).

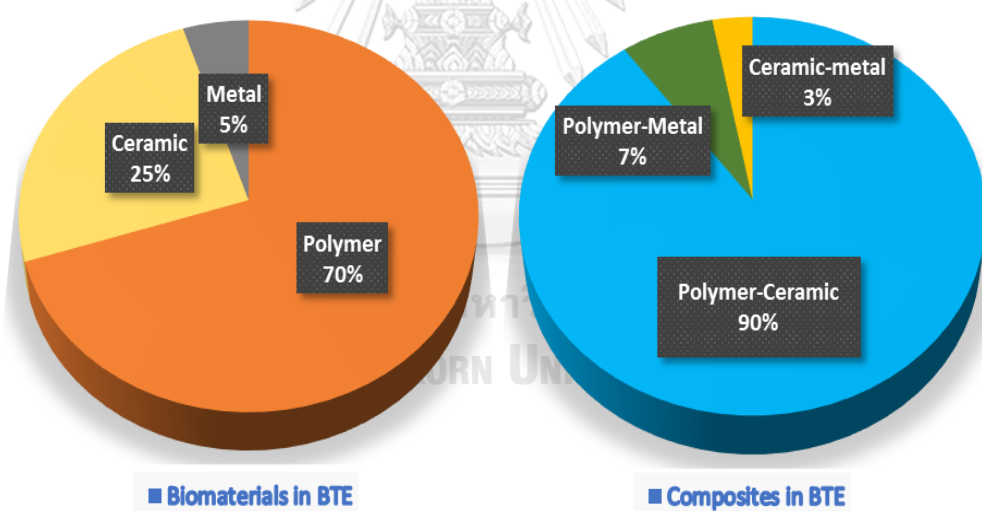


Figure 1 Proportion of scaffolds used in bone tissue engineering applications, pure biomaterials (A) and composites biomaterials (B).

Table 3 Type of biomaterials for scaffolds used in bone regeneration

Material type	Advantage	Disadvantage	Example materials
Metal	1. Good compressive strengths	1. Biomolecules cannot be integrated 2. Not biodegradable 3. Concerns about ion release	1. Tantalum 2. Titanium 3. Magnesium (alloy) 4. Iron (alloy)
Ceramic	1. Biocompatibility 2. Osteoinductive properties	1. Low fracture toughness 2. Difficulties in forming process	1. Bioglass 2. Calcium sulfate hemihydrate (CSH) 3. Calcium carbonate 4. Dicalcium phosphate 5. Octacalcium phosphate 6. β -Tricalcium phosphate 7. Biphasic calcium phosphate 8. Hydroxyapatite
Polymer	1. Biocompatibility 2. Easy formability 3. Good mechanical properties 4. Biodegradability	1. Low osteoinductive capacity	1. Polylactides (PLA) 2. Polyglycolides (PGA) 3. Polycaprolactone (PCL) 4. Cellulose 5. Hyaluronan 6. Fibrin 7. Collagen 8. Chitosan
Composite	1. Combine desirable properties of different materials		1. Amorphous CaP/PLGA 2. β -TCP/Chitosan/Gelatin 3. HA/Collagen 4. HA/PLGA

2.4 Chitosan for bone tissue engineering applications

Regenerative medicine faces new challenges in inducing tissue repair with naturally derived, highly biocompatible materials. Several studies proved that chitosan, a copolymer derived from chitin's deacetylation, is one of the most promising biopolymers for BTE. The chitosan's history began in the 19th century, Rouget et al. extracted the deacetylated form of chitin in 1859 (9). Chitosan has been proposed as a biomaterial for BTE applications for the past 40 years. Chitosan is a copolymer made of D-glucosamine and N-acetyl glucosamine units linked by β -glycosidic bonds (Fig. 2) (10).

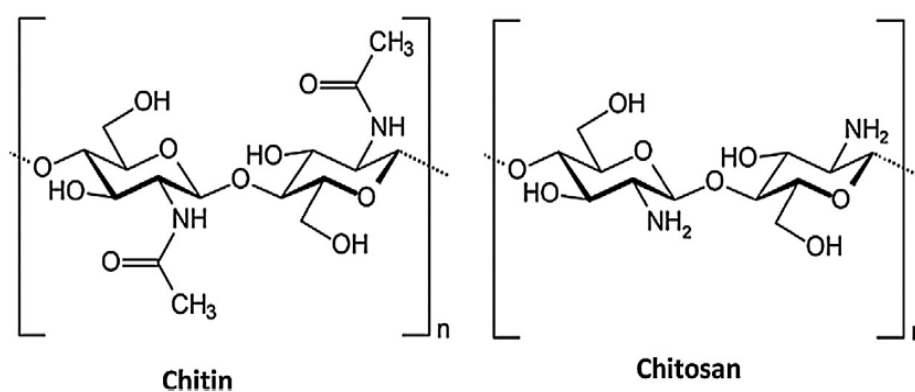


Figure 2 Chemical Structures of chitin and chitosan (10)

Chitosan is procured mainly from the exoskeleton of crustacean shells, including crab, shrimp, and corals (11, 12). Chitosan is the best form of chitin polymer due to its good biological properties, including soluble in organic acid, enhancing antibacterial and wound healing activities. Moreover, chitosan not only has significant osteoconductive properties but also has minimal osteoinductive properties (13-16). For bone engineering applications, Chitosan can also be prepared in different forms like sponges, fibers, films, and hydrogel. Therefore, chitosan shows most of the properties that make it is supporting its candidature for BTE applications (15, 17, 18).

In the fabrication process, previously, the most popular acid solutions used to dissolve chitosan and its derivative were monocarboxylic acids. Moreover, this method requires using a crosslinking agent such as glutaraldehyde for the formation of the scaffold. Besides monocarboxylic acids, there are many kinds of multi-carboxylic acids with more than one carboxyl group, such as acetic acid and formic acid. These multi-carboxylic acids are found to be naturally non-toxic solvents and are widely used in food and medical-related industries. Moreover, multi-carboxylic acids not only solubilize the chitosan in water but also improve the scaffold's property through its non-covalent cross-linking interaction with chitosan (19-21).

Recently, The Petroleum and Petrochemical College of Chulalongkorn University has investigated the rapid fabrication of chitosan scaffold using multi-functional carboxylic acids as nontoxic dissolving and cross-linking agents via conjugating reaction. This method was a green and simple fabrication method, with no unpleasant odor and significantly reduced contamination (22). However, our previous study shows that the mechanical properties of these polymer scaffolds do not provide sufficient structural support and dissolve faster than the rate of new bone formation *in vivo*. In order to improve the dissolution rate of pure chitosan scaffold, one solution is to incorporate other bioceramics into the polymer scaffolds to enhance mechanical strength and slow down the dissolution rate of the chitosan scaffold (23).

Similar results were observed using a porous membrane chitosan/hydroxyapatite membrane in a calvarial defect of rats. The results show that a composite membrane enhances new bone growth in the defect compared to a control. Together with the presence of osteogenic markers were more abundant in the experimental group (24).

Chitosan/calcium phosphate ceramics composite scaffolds have shown a relevant effect for BTE because of their ability to induce osteoblasts'

proliferation and showed good bone regeneration at eight weeks seen by micro computerized tomography in a tibial defect of rabbit (25).

2.5 Biphasic calcium phosphate ceramics for BTE applications

Nowadays, Calcium phosphate ceramics are the most popular ceramics used for bone tissue engineering due to their compositional structure similarities to adult human calcified tissues and the ability to bond with bone tissue (8, 26, 27). Synthetic calcium phosphate bone substitutes such as hydroxyapatite ($\text{Ca}_{10}(\text{PO}_4)_6(\text{OH})_2$) (HA), tricalcium phosphate ($\text{Ca}_3(\text{PO}_4)_2$) (TCP), and a combination of the two of these calls biphasic calcium phosphates (BCP) show more biocompatibility than many other ceramic and are common alternatives to autologous bone (28, 29). They mainly differ concerning their solubility or dissolution rate in acid solution, which may reflect their degradation *in vivo*. HA showed good osteoconductive ability and space maintenance properties; however, the disadvantages are very slow resorption rate (more than two years *in vivo*). β -TCP also exhibits excellent biocompatibility with osteoblasts but lower mechanical stability and faster degradable rate than the new bone formation rate. Therefore, a combination of HA and β -TCP in the form of biphasic calcium phosphate leads to a bone graft substituted with higher stability and lower degradability than other types of calcium phosphate ceramics. Moreover, numerous animal and clinical studies demonstrated that BCP has a new bone induction property more than pure HA or pure β -TCP (3, 30-32). However, BCP does not have osteoinductive properties by itself. But numerous studies have been proved that the osteoinductive property of BCP can be improved by combining BCP with other growth factors, bioactive proteins, or osteogenic drugs (26, 33, 34)

The properties mentioned above make BCP ceramics useful as a modifier of biodegradable natural and synthetic polymers to improve their

mechanical strength and decrease dissolution rates. Aylin et al. demonstrated that the addition of BCP to porous chitosan scaffolds could enhance new bone formation *in vitro* (35). Padalhin et al. developed a chitosan/Gelatin BCP bi-layer composite scaffold. This novel scaffold can be used as hemostat material and enhance new bone formation in rat skull defects (36).

2.6 Epigenetic

Epigenetics refers to heritable mechanisms changes in gene expression that do not involve changes to the underlying DNA sequence of genes. Many studies reported a wide variety of health indicators that have some level of evidence implicating epigenetics.

Any external stimulus such as illnesses and behaviors that the body can detect has the potential to cause epigenetic modifications. Epigenetics can be passed from parents to offspring, referred to as epigenetic inheritance (37). There are three main mechanisms of epigenetics: chemical modifications of DNA itself, called DNA methylation, the modification of histones protein around the DNA, and regulation of gene expression by non-coding RNA.

The biology of cells is partly based on epigenetic regulation (38, 39). Chromatin is the complex of a mass of genetic material composed of proteins and DNA that is tightly condensed to fit within the nucleus of eukaryotic cells. The fundamental unit of chromatin, called the nucleosome, each nucleosome composed of DNA sequence (~ 150 basepairs) wrapped around a set of eight protein subunits called histones. Two copies of four histone types, H2A, H2B, H3, and H4, make up the octamer, which left-handed superhelix wraps ~ 1.7 turns of DNA. Histone modification processes are the covalent post-translational modification. The two distinctive groups modifying enzymes involved in histone modification are histone acetyltransferases (HATs) and

histone deacetylases (HDACs). HATs catalyze the acetylation of conserved lysine residues on histone proteins by transferring an acetyl group which can open chromatin structure and correlates to gene activation. However, HDACs can remove acetyl groups from an ϵ -N-acetyl-lysine on histone, resulting in chromatin condensation related to transcriptional repression (40).

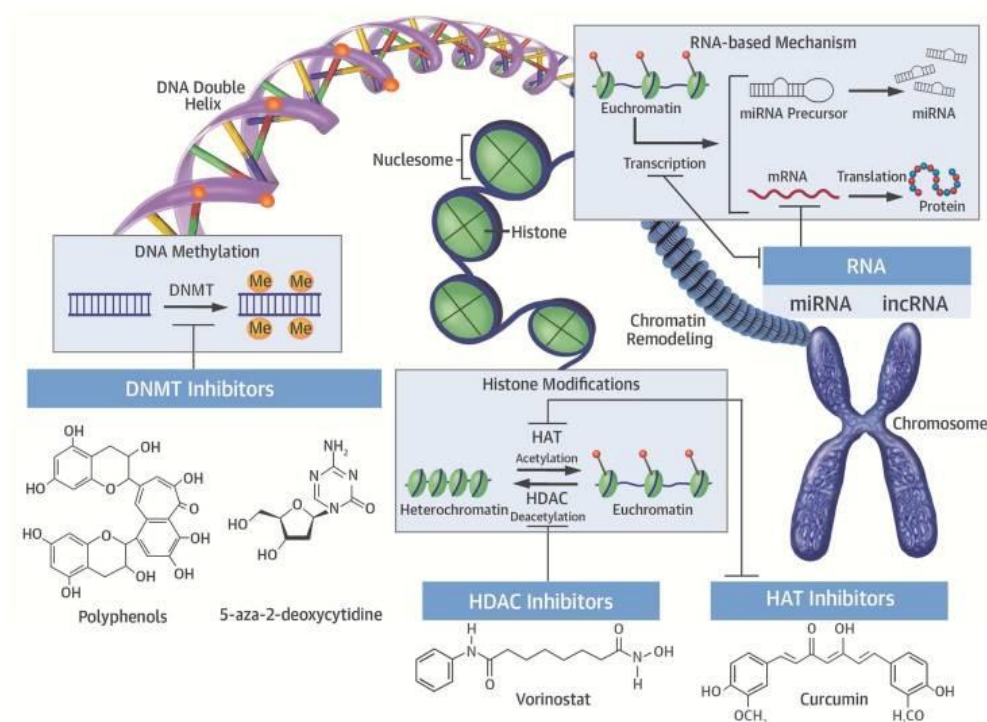


Figure 3. Epigenetic mechanisms (Reprinted from J Am Coll Cardiol. 2017 Aug 1; 70(5): 590–606. with permission from PMC) (41)

2.7 Epigenetic Regulation of Bone remodeling

Bone remodeling is defined as a continuing complex biological process of synthesis and destruction of skeleton tissue trying to maintain the structural and biological integrity of the bone. Epigenetic regulation plays an essential role in coordinating the behavior and activities of many types of bone cells. Recently, several pieces of research have been focusing on the relationship

between epigenetic modification by regulating HDAC enzymes and the bone remodeling process.

In humans, there are 18 HDAC enzymes divided into four classes of compounds according to HDAC homology (42) (Table 4). One approach targeted to epigenetic changes is using histone deacetylase inhibitor (HDACI), which has antitumorigenic effects, including growth arrest, apoptosis, and the induction of cell differentiation. In the past, HDACI is often seen used in neurology as mood stabilizers and anti-epileptics. Some HDACIs are currently approved by the FDA or clinical trials for cancer and inflammatory disease treatments. HDACI work by blocking the action of several types of HDAC resulting in enhanced acetylation of core histones, leading to an open chromatin structure that correlates to gene activation.

Table 4. HDAC classification (43).

Group	Class	Name	Location in cell
Classical (Zn dependent)	Class I (Rpd3)	HDAC1	Nucleus
		HDAC2	Nucleus
		HDAC3	Nucleus
		HDAC8	Nucleus
	Class IIa (Hda1)	HDAC4	Nucleus/cytoplasm
		HDAC5	Nucleus/cytoplasm
		HDAC7	Nucleus/cytoplasm
		HDAC9	Nucleus/cytoplasm
	Class IIb (Hda1)	HDAC6	Cytoplasm
		HDAC10	Cytoplasm
Class IV	HDAC11	Nucleus/cytoplasm	
NAD-dependent	Class III	SIRT1-7	Nucleus/cytoplasm

It has been suggested that HDACi can be used to regenerate different types of tissues such as bone, cartilage, cardiac, liver, and skin (44, 45). Trichostatin A (TSA), a natural derivative of dienohydroxamic acid produced by *Streptomyces* sp. TSA is a broad-spectrum HDAC inhibitor, which is potent and pans specifically inhibitor of HDAC class I/II (46). There are many studies about the effects of TSA because it reversibly inhibits HDAC in low nanomolar concentrations compared with other known HDAC inhibitors. Current reports have demonstrated that TSA can induce osteogenic differentiation of human periodontal ligament cells by inducing hyper-acetylated histone H3 during the differentiation process. Besides the inhibition of HDAC, TSA also enhanced *in vivo* bone regeneration in mice calvarial bone defect model (47-49). Meanwhile, Inhibition of HDAC 1 and 2 have presented favorable inhibition of osteoclast bone resorption *in vitro* (50, 51). In addition, Zhang et al. reported that TSA incorporated aligned fibers of the PLLA scaffold can directly induce tenogenic differentiation of tendon stem cells *in vitro* and promote the structural and mechanical properties of the regenerated Achilles tendon in a rat model (52). Moreover, Lee et al. reported that when collagen scaffolds soaked with HDAC inhibitor solution were implanted in the mouse calvarial defect model, the improvement in bone formation and inhibited bone resorption were observed (53). This evidence has demonstrated the possibility of using HDACi as a growth factor to induce new bone formation in the bone regeneration process.

CHAPTER 3 MATERIAL AND METHODS

3. Material and Methods

3.1 Fabrication of CS/BCP/TSA scaffold

4% w/v of medium-molecular-weight chitosan (Mw: 250 kDa, Particle size: 0.5 μ m, \geq 90% deacetylated, Marine BioResources, Thailand) was dissolved in succinic acid solution and stirred overnight at 60 °C. The different amounts of BCP (Particle size: 0.1 - 0.5 μ m, MTEC, Pathumthani, Thailand), 10%, 20%, 40% w/w, and TSA (Sigma-Aldrich, Oakville, Canada) 200, 400, 800, 1600 nM were added into chitosan (CS) solution. To prepare a CS hydrogel, the 1-(3-Dimethylamino-propyl)-3-ethyl carbodiimide hydrochloride (EDC)/N-Hydroxysuccinimide (NHS) molar ratio was set as 1:1. Finally, hydrogels were freeze-dried at -50°C for 48 h to obtain CS/BCP/TSA scaffold. The fabrication method and gross scaffold structure are shown in Figures 4A and 4B.

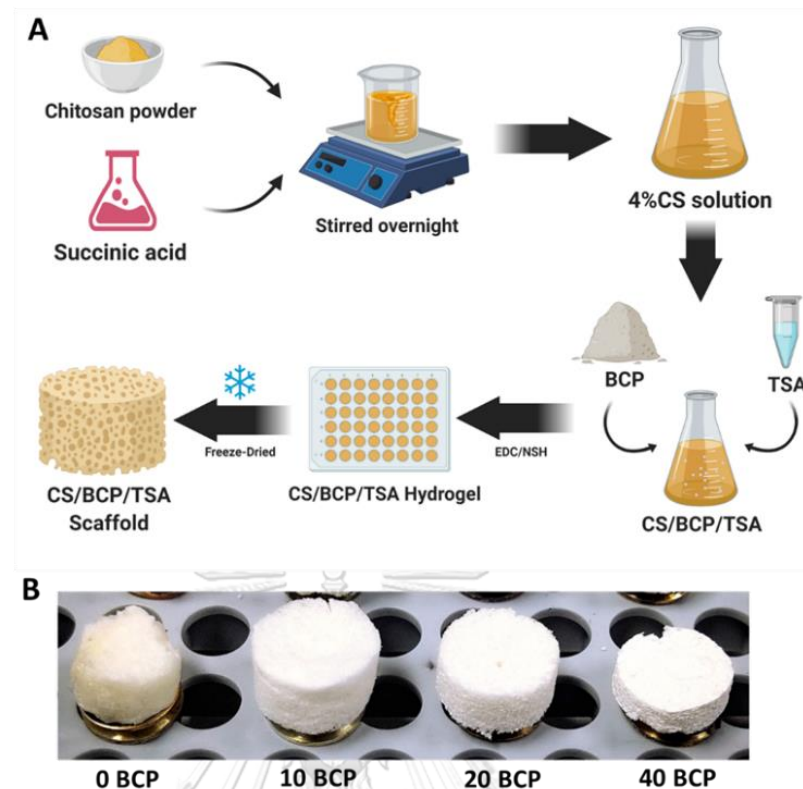


Figure 4. CS/BCP/TSA scaffold fabrication. (A) A schematic illustration of scaffold fabrication with freeze-drying technique. (B) Scaffold architectures: 0% BCP, 10% BCP, 20% BCP, and 40% BCP

3.2 Culture of primary human periodontal ligament cells

With informed consent, the hPDLs were obtained from the extracted healthy third molars of young individuals aged 18–25-year-old (Appendix for details of hPDLs culture). All procedures were performed under the approval of the Ethical Committee of the Faculty of Dentistry, Chulalongkorn University, Thailand (Approval Number: HREC-DCU 2020-106). The third molars were washed, and the soft tissue attached to the cervical area was removed. Then the periodontal ligament attached to the central one-third of the root surface was carefully scraped off. Tissue samples were seeded in a culture medium (10% FBS, 1% L-Glutamine, and 1% antibiotics in DMEM, Gibco). The cells were

incubated at 37° C humidified atmosphere with 5% CO₂. The hPDLCs in the third to fifth passage were used in this study.

3.3 Characterization of the CS/BCP/TSA scaffolds

3.3.1 Physical and chemical characterization of the scaffolds

The CS/BCP/TSA scaffolds were prepared into a cylinder shape (10 x 8 mm). FTIR was conducted using a Perkin-Elmer spectrometer for analyzed the chemical contents of the scaffolds in the standard frequency range (4000–400 cm⁻¹). The surface morphologies of the scaffolds were observed by scanning electron microscope (SEM) and evaluated by image visualization software (Image J, NIH, USA). The mean pore size and pore size distribution were calculated on random 10 mm² of SEM images based on 100 pores. Water uptaking ability was investigated by immersing the scaffold in phosphate-buffered saline (PBS) and calculating the weight change after immersion at 0, 5, 30 min, 1, 12, and 24 h. All measurements were performed in triplicate.

3.3.2 *In Vitro* Degradation of Scaffold

The *in vitro* degradation behavior of the CS/BCP/TSA scaffolds was investigated by monitoring the weight change of the scaffolds after immersion in 1 mL phosphate-buffered saline (PBS) containing 1.5 μg mL⁻¹ lysozyme (hen egg-white, Sigma–Aldrich, Oakville, Canada) at 37 °C in a shaker. To continue the enzymatic activity, the lysozyme was refreshed daily. At the time intervals of 3, 7, 14, 30, 60 and 90 days, the scaffolds were washed with distilled water, freeze-dried, and then weighed (W_d).

3.3.3 *In vitro* release and bioactivity of TSA from CS/BCP/TSA scaffolds

In vitro release of TSA was determined by incubating 20 mg of scaffolds in 25 mL of PBS separately maintained in the shaker (60 rpm) at the

physiological condition for 28 days. At the time intervals of 1, 3, 7, and 28 days, 1 mL of the samples were collected and analyzed using at 280 nm with a using UV-Vis spectrophotometer. A standard curve of pure TSA in a standard solution ranging from 0 to 1600 nM was constructed. The cumulative release of TSA from the CS/BCP/TSA scaffolds at each time interval was calculated and expressed as a percentage of initial loading.

The bioactivity of TSA that was released from CS/BCP/TSA scaffolds was evaluated by determining its HDAC activity with the fluorometric HDAC Activity Assay kit (Abcam, Cambridge, MA). Briefly, hPDLs were treated with 1 mL of supernatant collected from the scaffolds and incubated for 72 h. The cell lysates were incubated with substrate peptide for 30 min on a microtiter plate. Then the developing solution was added to each well for a further 20 min. The reaction was stopped by adding the stop buffer, and the fluorescence intensity at Ex/Em = 350/460 nm was measured in a fluorescence plate reader.

3.3.4 Mechanical properties

The compressive modulus of the scaffolds in both the dry and wet state were determined using a universal testing machine (Instron, Japan). The compression rate was set at 2 mm/min, and the load was applied until the samples were pushed to approximately 80% of their original shape. All samples were performed in triplicate.

3.4 *In vitro* biocompatibility analysis

3.4.1 Cellular biocompatibility

According to the MTT assay, the viability was measured on both hPDLs and MC3T3-E1 cells. The CS/BCP/TSA scaffolds and commercial bone graft

products (Osteon III collagen, Dentium, Seoul, Korea) were sterilized under UV light for 30 min. For the direct contact test, hPDLCs 5×10^3 cells/well were cultured on a well plate for 24 h, then placed a scaffold on top of the monolayer cells and incubated for 0, 1, 4, and 7 days. For the indirect contact test, a small piece of scaffold (0.2 g/ml) was immersed in a culture medium for 24 hours at 37°C. The supernatant obtained was applied to the monolayer culture of MC3T3-E1, incubated for 0, 1, 4, and 7 days, then added 10 μ l of MTT per well with a subsequent incubation for two h. and measured the absorbance at 570 nm. The cells cultured without scaffold were served as a control.

3.4.2 Cells attachment and morphology on the scaffolds

The attachment and morphology of hPDLCs in scaffolds at 48 h were observed by using SEM. The 10^5 hPDLCs were seeded onto a scaffold and incubated for 48 hours. Before observing cell adhesion, the samples were rinsed three times with PBS to eliminate any unattached hPDLCs and fixed in 2.5% glutaraldehyde. Then, samples were dehydrated in a gradient ethanol series and dried at room temperature.

3.4.3 Real-time reverse transcription-polymerase chain reaction (RT-PCR)

To estimate the effect of CS/BCP/TSA scaffolds on the expression of the inflammatory-related gene and osteoblast-related genes by hPDLCs, quantitative real-time PCR was performed. hPDLCs were incubated with CS/BCP/TSA scaffolds and commercial bone graft products for 5 and 10 days in an osteogenic medium. Details of the PCR primers used are described in table 4. All samples were performed in triplicate.

Table 4. The primer sequences of the upstream and downstream primers for these mRNA analyses (5' to 3').

IL-1 β	TGGACCTTCCAGGATGAGGACA	GTTTCATCTCGGAGCCTGTAGTG
COL-1	GTGCTAAAGGTGCCAATGGT	ACCAGGTTACCCGCTGTTAC
RUNX2	CCCCACGACAACCGCACCAT	CACTCCGGCCCCACAAATC
ALP	CGAGATACAAGCACTCCCACTTC	CTGTTTCAGCTCGTACTGCATGTC
OPN	AGGAGGAGGCAGAGCACA	CTGGTATGGCACAGGTGATG

3.5 *In vivo* bone regeneration potential

The animal procedure was modified from our previous study (54), which was approved by Chulalongkorn University Animal Care and Use Committee (CU-ACUC), Thailand (Animal Use Protocol No. 2073032). Twenty-four 8-week-old C57BL/6 mice were anesthetized with intraperitoneal injection of Zoletil100 (40 mg/kg) and xylazine (5 mg/kg). Two bilateral full-thickness calvarial defects (4mm in diameter) were created using a biopsy punch (Stiefel, GSK, NC, USA). Mice were randomly divided into four groups as follows: (1) CS/BCP scaffold, (2) CS/BCP/TSA scaffold, (3) commercial bone graft products as a positive control, and (4) empty defects as a negative control. A schematic illustration and surgery steps of the procedure are shown in Appendix Figure 1.

After being euthanized at 6 weeks and 12 weeks, samples were excised and fixed in 10% buffered formalin. The mineral density and the morphology of the defects were evaluated by a micro-CT scanner (SCANCO Medical AG, μ CT 35, Switzerland). The samples were decalcified and embedded in paraffin and were then cut along the larger diameter of the defect. Sections at ten μ m each were stained with hematoxylin and eosin (H&E) and Masson's Trichrome.

3.6 Statistical Analysis

The statistical analysis was performed with SPSS 23 (IBM, New York, USA) using the One-Way Analysis of Variance (ANOVA) test for both *in vitro* and *in vivo* studies. Significant differences were indicated as: *($P < 0.05$) for significant and ** ($P < 0.01$) for highly significant differences.



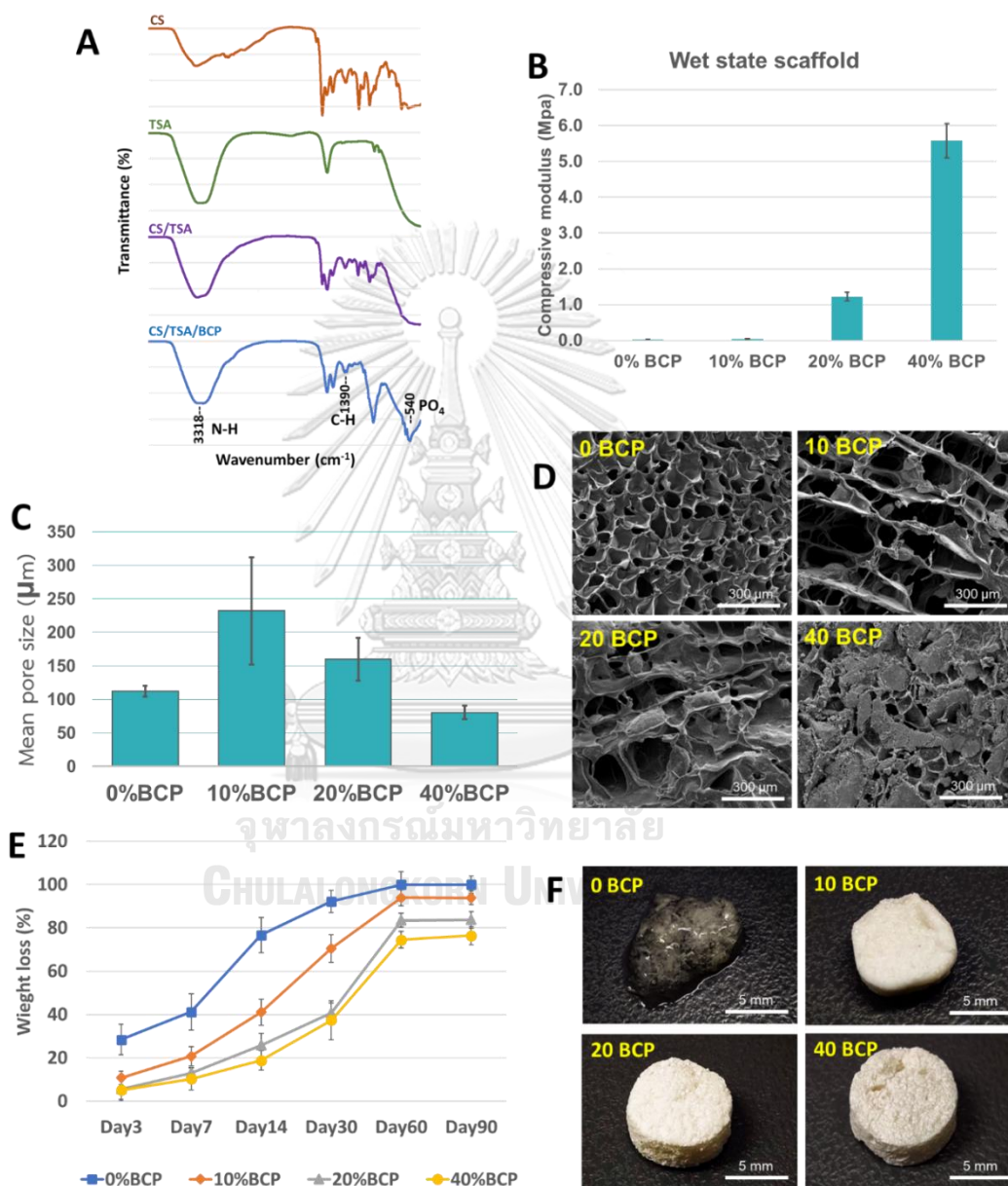
CHAPTER 4 RESULTS

4.1 Selection of optimal physicochemical scaffold

The CS/BCP/TSA scaffolds with cylindrical shapes were successfully constructed by freeze-dried technique, as shown in Fig. 4A. The morphology of scaffolds in different proportions of BCP was shown in Fig. 4B. The BCP microparticles were homogeneously blended with the scaffold structure. FTIR spectra of CS, TSA, CS/BCP, and CS/BCP/TSA scaffolds were presented in Fig. 5A. In the CS/BCP/TSA scaffolds sample, C-H bending appears at the FT-IR absorption peak at 1390 cm^{-1} , indicating the presence of CS. In contrast, the absorption peak at 540 and 600 cm^{-1} (between the ceramic and polymer matrix) demonstrated characteristics of PO_4 bands of BCP. Moreover, successful TSA incorporation in the bio-ceramic matrix was confirmed when applying an absorption peak at 3318 cm^{-1} to N-H stretching of TSA.

With the addition of BCP, the compressive strength of the scaffolds was increased in both wet states compared to the pure CS scaffold (Fig 5B). Physiologically, the scaffold for bone regeneration was constantly exposed to body fluids in its clinical use; therefore, the mechanical strength evaluated after fluid immersion more closely mimics the stage of the scaffold *in vivo*. SEM images showed an interconnected porous network in the scaffold of all groups except for the 40% BCP group, which presented low porosity and dense structure. Also, the BCP particles were homogeneously distributed on the scaffold pore's wall (Fig 5D). The average pore sizes of the scaffolds were 110 ± 6 , 232 ± 160 , 160 ± 52 , and $88 \pm 10\ \mu\text{m}$ for 0%, 10%, 20%, and 40% proportion of BCP, respectively (Fig 5C). The degradation behavior of the scaffolds in a solution containing lysozyme showed that pure CS scaffold

degraded very fast by losing more than 80% of its original weight within 30 days. By increasing the BCP proportion, the scaffolds could maintain an interconnected porous structure while dramatically reducing the degradation rate (Fig 5E, 5F). From all physical and chemical characteristics, the 20% BCP



scaffold was used for subsequent experiments.

Figure 5. Physical characterization of CS/BCP/TSA scaffolds in various BCP proportions. (A) FT-IR spectra of CS/BCP/TSA scaffolds showed the absorption peak at 540, 600, 1390, and 3318 cm⁻¹, representing each scaffold

compartment. (B) With the increase in BCP proportion, the compressive strength of the scaffolds in the wet state was increased. (C) The mean pore size of CS/BCP/TSA scaffolds in various BCP proportions. (D) The SEM surface morphology of CS/BCP/TSA scaffolds in various BCP proportions. (E) The enzymatic degradation behavior of CS/BCP/TSA scaffolds. (F) The gross structure of CS/BCP/TSA scaffolds before freeze-drying at 30 days after enzymatic degradation.

4.2 Cytocompatibility and Cytotoxicity

The MTT assay was used to evaluate the effect of the synthesized scaffolds on hPDLCs and MC3T3-E1 cell viability for direct contact and extracted method, respectively, shown in Fig. 6. Both methods showed a similar trend of the results, which indicated that all samples positively affected hPDLCs and MC3T3-E1 cell viability. Moreover, the results clearly showed that the number of viable cells significantly increased in 400 and 800 nM of TSA-containing scaffolds after four days of culturing. However, 1600 nM of TSA-containing scaffolds significantly decreased the cell viability at all time points, indicating cytotoxicity. SEM evaluated the attachment and morphology of hPDLCs culture for 48 h on the samples. hPDLCs exhibited good adhesion on the scaffold surface of all groups and a positive control sample (Fig. 7A). Interestingly, the cells seeded on a higher concentration of TSA-containing scaffolds displayed numerous pseudopod protrusions to contact adjacent cells.

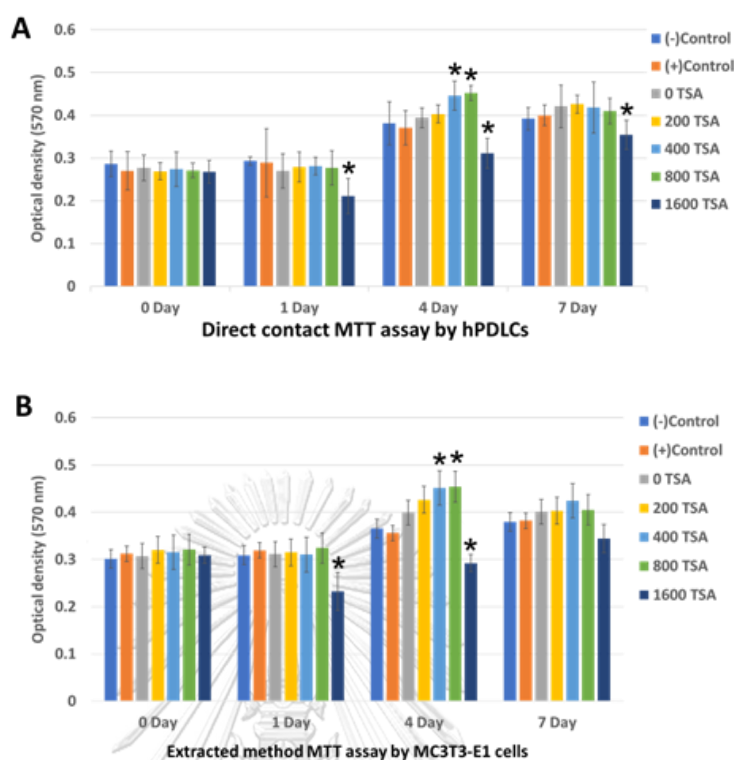


Figure 6. Biological properties of CS/BCP/TSA scaffolds in various TSA concentrations. (A) Cytocompatibility of CS/BCP/TSA scaffolds in different TSA concentrations by direct contact method with MTT assay. (B) Cytocompatibility of CS/BCP/TSA scaffolds in various TSA concentrations by extracted method with MTT assay.

4.3 Cytocompatibility and Cytotoxicity

To test the bioactivity of TSA in the scaffolds, TSA concentrations were set to 0, 200, 400, 800, and 1600 nM and measured at predetermined time points. Fig. 7B showed a linear increase in TSA cumulative release during the first five days. A similar trend of initial rapid release of TSA was found within 24 h, followed by gradual release up to 50% within three days. After 5 d, the TSA was completely released from the scaffolds. The cumulative releases of TSA were approximately 40%, 42%, 54%, and 57% in 200, 400, 800, and 1600 nM groups, respectively. The HDAC activity in the nuclear extracts of hPDLCs was 4

to 5-fold lower than in the control (Fig. 7C). TSA concentration as low as 200 nM was able to inhibit HDAC activity. However, no significant difference in HDAC activities was observed among all TSA incorporated groups. This result confirmed that TSA released from the scaffolds could inhibit HDAC activity of hPDLCs

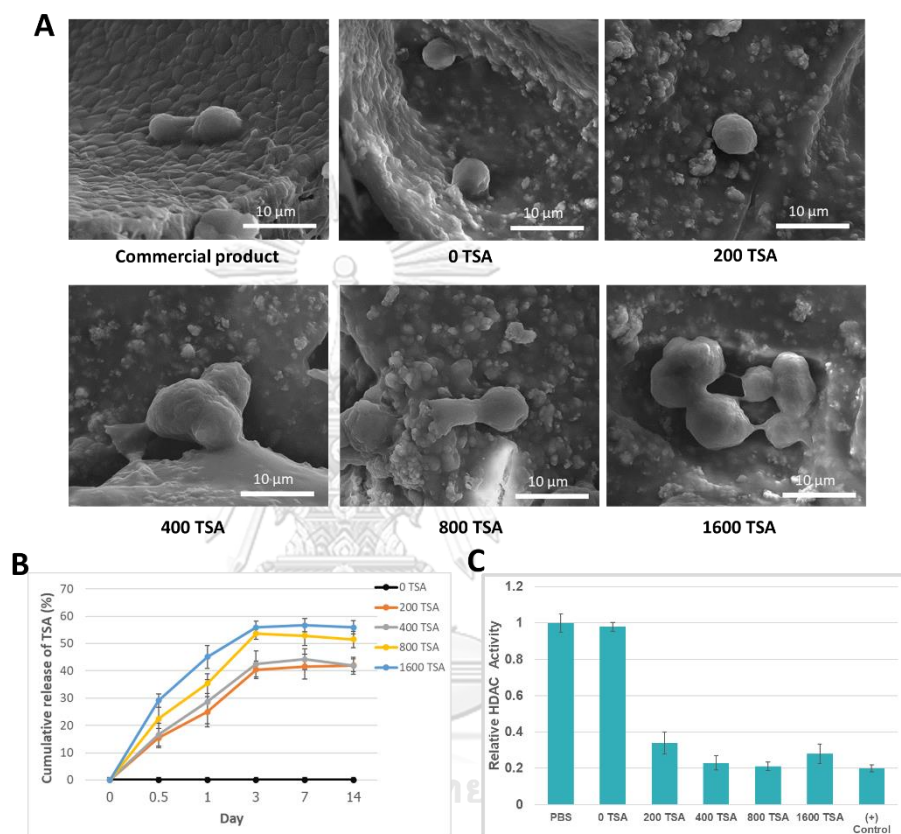


Figure 7. Cells attachment and Drug Released abilities (A) SEM microphotographs of the hPDLCs cultured on CS/BCP/TSA scaffolds in various TSA concentrations. (B) Cumulative release curve of TSA. (C) The HDAC activity of hPDLCs treated with conditioned media of CS/BCP/TSA scaffolds.

4.4 Expression of inflammatory and osteogenic genes

The influence of CS/BCP/TSA scaffolds on inflammation and osteoblast differentiation was investigated by observing genes expression for 5 and 10 days. The results confirmed that the newly fabricated scaffolds and commercial bone graft do not stimulate IL-1 β , an inflammatory-related gene.

While most of the osteoblast-related genes, including Runx2, COL1, ALP, and OPN were significantly induced by CS/BCP/TSA scaffold. After five days of culture, RUNX2, a master gene controlling osteoblast differentiation, showed a marked increased expression. OPN, late markers of differentiated osteoblasts, was highest after ten days of culture. COL1, the most abundant extracellular matrix protein in bone, and ALP, an early marker for osteoblast differentiation, were significantly upregulated at both time points (Fig. 8).

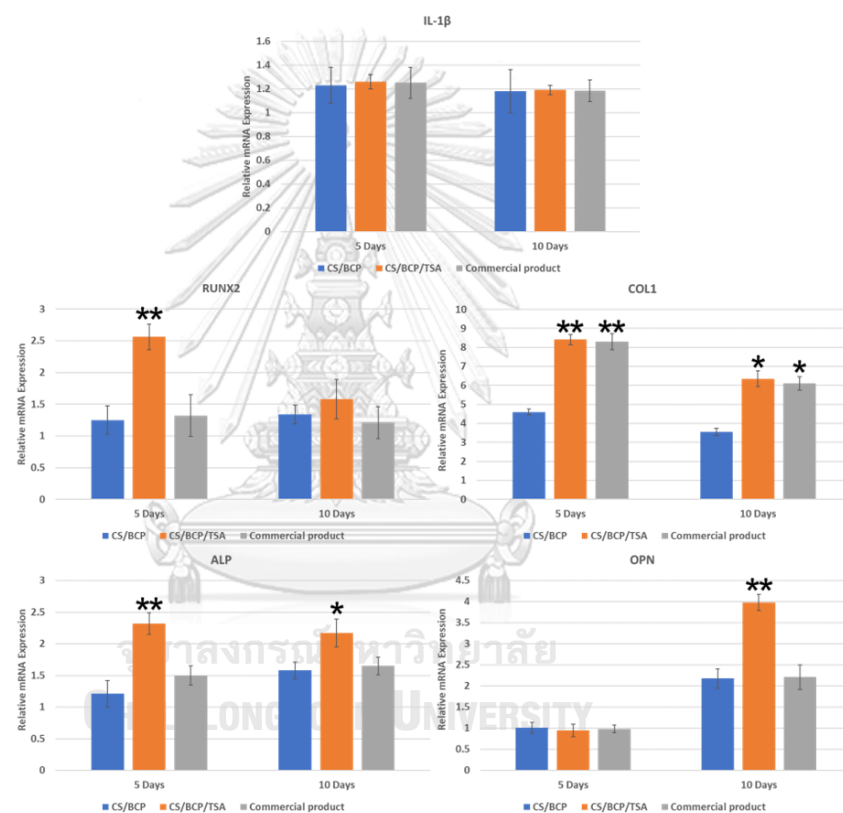


Figure 8. Expression of inflammatory and osteogenic genes of hPDLCs after cultured with CS/BCP/TSA scaffolds for 5 and 10 days, compared with CS/BCP without TSA loading and commercial bone graft product.

4.5 *In vivo* bone regeneration

Micro-CT was used to evaluate the mineralized content in mouse calvarial defects. At six weeks post-implantation, 3D constructed images showed hard tissue formation in newly fabricated scaffolds groups and the

commercial product group. In contrast, hard tissue formation in the defects for the sham group was not detected. After 12 weeks, new hard tissue formation was seen throughout the defects, especially the in-growth of new bone from the periphery of the defect in the CS/BCP/TSA scaffold group compared to other groups (Fig 9A). Although quantification of BV/TV demonstrated that the commercial product group has the highest BV/TV at 6-week, however CS/BCP/TSA scaffold group showed a marked increase in the amount of BV/TV at 12-weeks (Fig 9B).

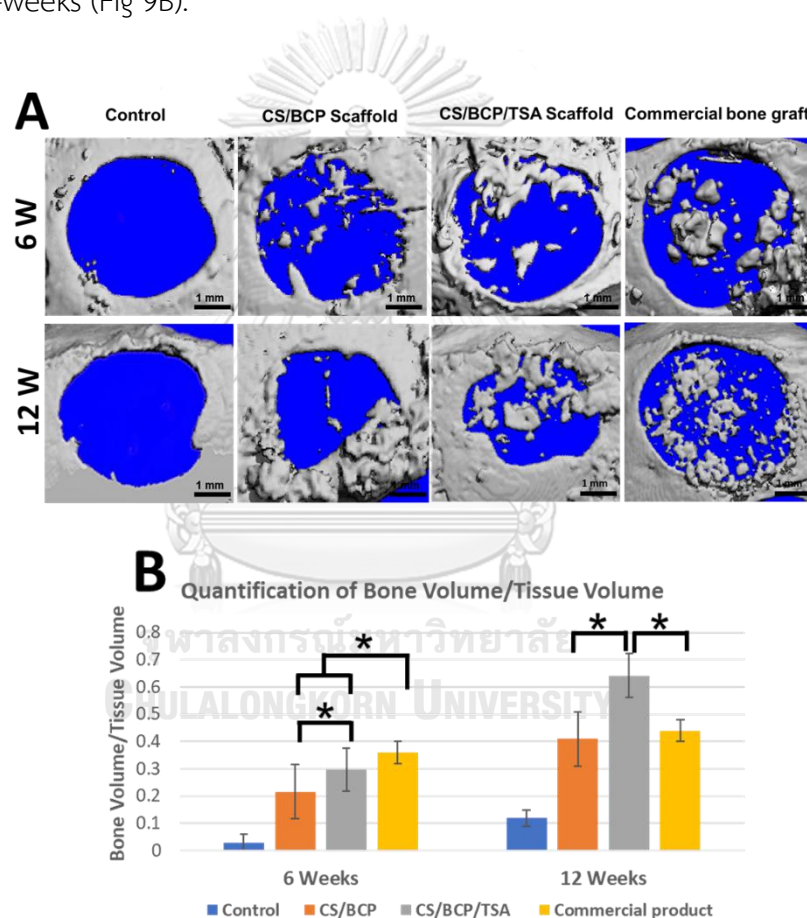


Fig. 9. *In vivo* bone regeneration potential of CS/BCP/TSA scaffolds. (A) Micro-CT-based 3D images of new bone formation (Scale bar – 1 mm). (B) Quantification of BV/TV of CS/BCP/TSA scaffolds, compared with CS/BCP without TSA loading and commercial bone graft product at 6 and 12 weeks after implantation.

The histological analysis of sections stained with H&E and Masson's trichrome is shown in Fig. 10 and Fig. 11. At six weeks, the new bone formation started from the peripheral region of all implanted groups. The CS scaffold groups showed thick connective tissue with osteoid deposition. The trabeculae-like structure implied mature bone was found in the defect implanted with CS/BCP/TSA scaffold at as early as six weeks. Commercial graft implantation obviously showed the incomplete degradation of BCP particles surrounding by fibrous tissue. At 12 weeks, organized mature lamellar bone was more apparent in the defect of the CS/BCP/TSA scaffold group. The negative control group showed a thin layer of connective tissue with no bone formation at either time point.

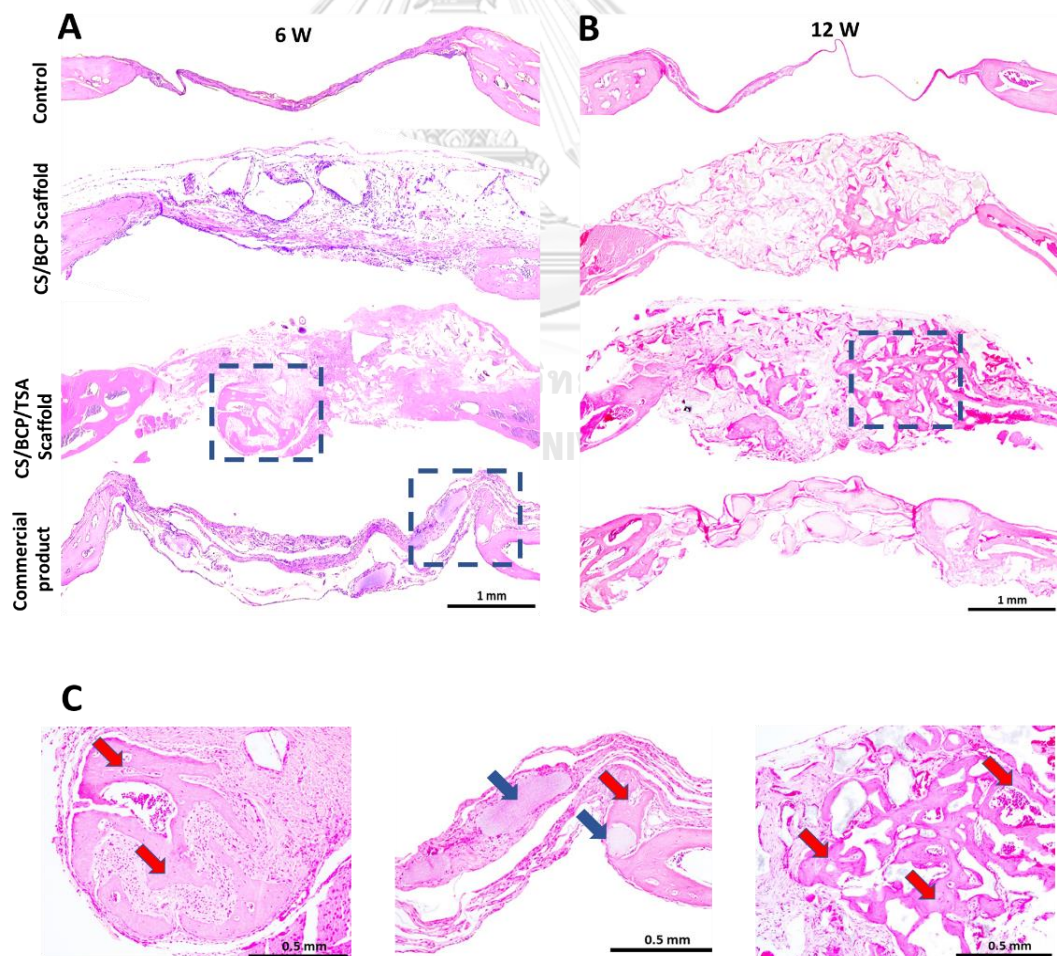


Figure 10. By H&E staining, (A) Histological view of defects implanted with scaffold at 6 and 12 weeks after implantation, low magnification (10×), scale bar – 1 mm. (E) High magnification (40×), from left to right panels, showing the trabecular bone ingrowth in CS/BCP/TSA scaffolds both 6 and 12 weeks (red arrows), while commercial graft group remains incompletely BCP resorption (blue arrows), scale bar – 0.5 mm.

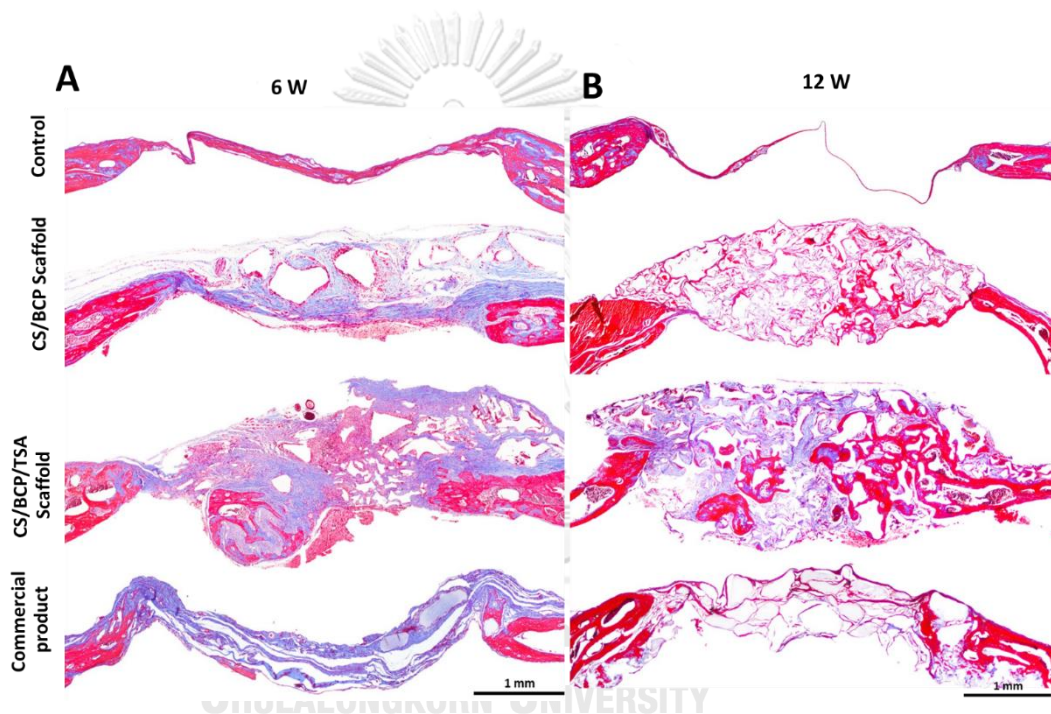


Figure 11. By Masson's trichrome staining, histological view of defects implanted with scaffold at 6 and 12 weeks after implantation, low magnification (10×), scale bar – 1 mm.

CHAPTER 5 DISCUSSION

In the present study, highly porous CS-based scaffolds were fabricated using a freeze-drying technique. First, we worked to identify the proportion of BCP which showed the most suitable biomechanical properties. The results indicated that the physicochemical characterizations of CS scaffold (Pore size, degradation rate, and mechanical strength) were significantly improved by incorporating BCP. Previous studies have shown that heterogeneous pore sizes in the range of 100–325 μm with a high degree of distribution are optimal for bone scaffolds (55). The optimal proportion of interconnected pores should be used somewhere in the range of 100–200 μm for maximum cell adhesion and proliferation. In contrast, a faster rate of neovascularization is achieved through the small fraction of the larger porous structure ($> 300 \mu\text{m}$). The degradation rate should be equal to regenerated bone (56). Additionally, optimal compressive strength of bone scaffold is achieved when given in the range of 1–12 Mpa for the provided 3D matrix, which allows the proliferation of osteoinducible cells (57, 58). All our testing results proved that CS-based scaffolds with 20% of BCP meet or exceed the minimum requirements of physicochemical performance for bone tissue engineering scaffolds. This phenomenon is attributed not only to the formation of a strong network penetration of BCP particles into the surface of CS networks but also to strong ionic interaction between PO_4^{3-} in BCP with NH_3^+ in CS (59, 60).

The present study is the first experimental evidence for incorporating the epigenetic modulation molecule into the bone regeneration scaffold. In response to environmental and metabolic activities, epigenetic processes regulate the modulation of gene expression via microRNA regulation, DNA methylation, or histone modification (61, 62). Furthermore, previous studies have proven that TSA, an epigenetic modifier has a beneficial effect on bone

repair and regeneration. Li et al. reported that TSA could promote osteogenic differentiation of mesenchymal stem cells by inhibiting the nuclear factor- κ B (63). Additionally, our studies confirmed that TSA has the ability to induce osteogenic differentiation of hPDLCs and demonstrates a potential application of TSA for bone regeneration therapy (47, 49). The results show that the TSA release profile can be divided into two phases. Phase 1: TSA had an initial burst within 24 h. Phase 2; (24 h-3 d), TSA sustained release from the scaffolds at 55%. These phenomena might result from the weak hydrogen bond between the hydrophilic part of the TSA molecule and the hydroxyl group of CS. Notably, the total amount of TSA released from 800 nM TSA scaffold was calculated to be 435 ± 16 nM, which showed excellent biocompatibility and enhanced hPDLCs and MC3T3-E1 cell proliferation. Whereas the 1600 nM TSA scaffold showed toxicity with the cells. These data corresponded with our previous study (Huynh et al. 2016) that the optimal concentration of TSA to induce osteogenic differentiation without cytotoxicity is 400 nM. The CS/BCP scaffolds act as a suitable carrier, providing a sustained release ability for TSA. The CS/BCP/TSA scaffold with 20% of BCP and 800 nM of TSA was determined to be the optimal proportion to provide mechanical and biological properties to support bone formation.

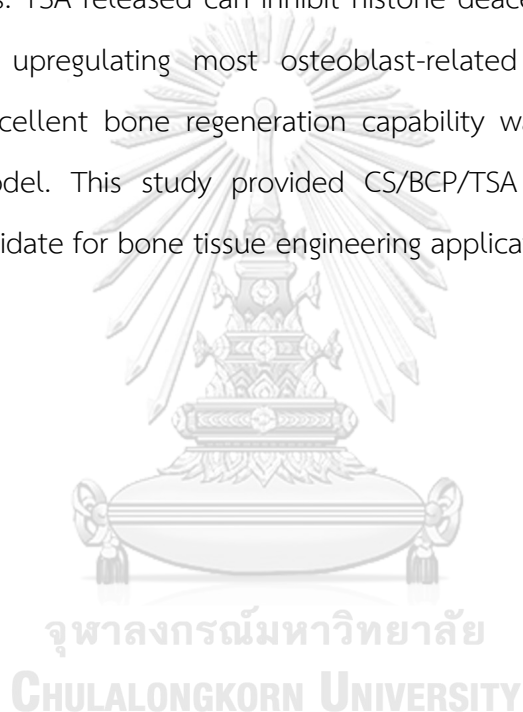
One limitation of this study is the lack of evidence about the optimal exposure time of TSA for maximizing bone regeneration. Compared to the bone healing processes, the first three-day in the healing period might be too early for inducing the interplay of osteoprogenitor cells. This phenomenon is explained due to weak non-covalent immobilization between TSA molecules and the polymeric chain of CS. Evidence has shown that microfabrication techniques such as 3-dimensional printing or electrospinning and using a microsphere release system can enable drug molecules to sustain release in sequential manners (64). Further studies should be conducted to modify the

fabrication procedure and TSA loading method, resulting in a controlled release fashion.

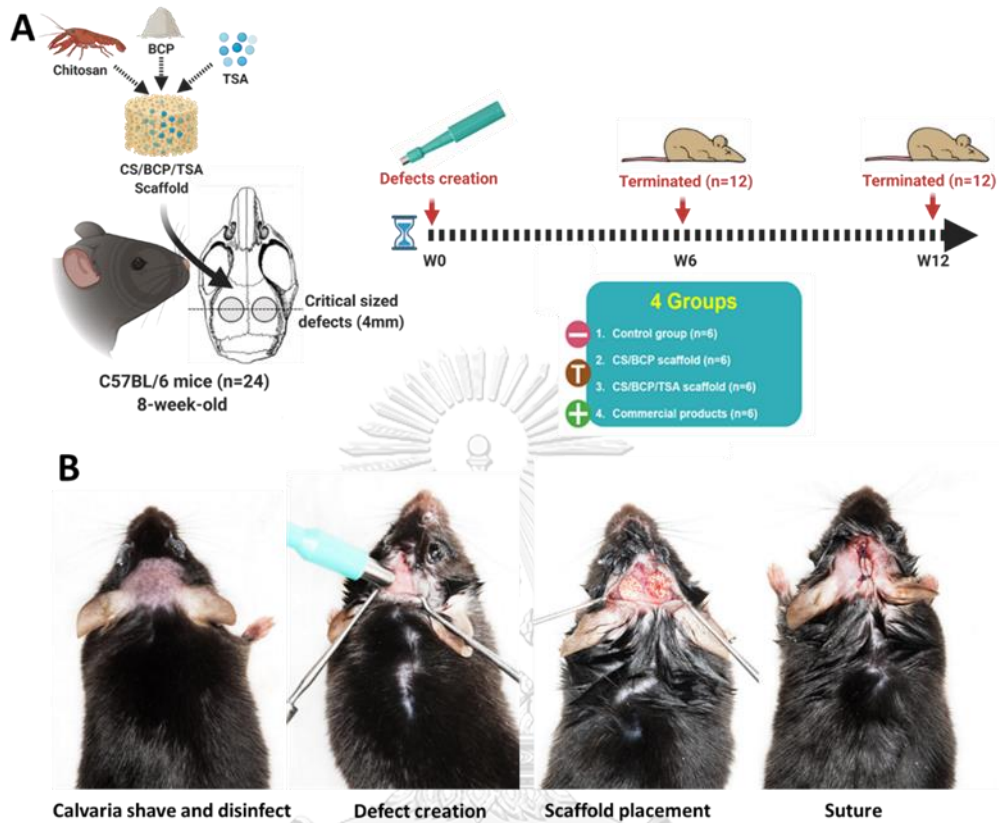
At six weeks, our *in vivo* results demonstrated a significant increase in BV/TV in the defects implanted with CS/BCP scaffold with or without TSA and commercial bone graft. The commercial bone graft showed the highest BV/TV at this time point. These phenomena might result from incompletely degraded BCP, which is a major mineralized content in the scaffold. This evidence was clearly seen in histology results. Notable increases in bone formation were found in scaffolds loaded with TSA at the 12-week time interval. Remarkably, histological analysis reveals that trabeculae-like structure seamlessly continues with pre-existing bone in the defects implanted with CS/BCP/TSA scaffold at both time points. This result corresponded with the previous study (65) that TSA is a potent osteogenic inducer and can enhance bone formation in an animal model. The *in vivo* results confirmed that the CS/BCP/TSA scaffold possesses excellent osteogenic bone tissue engineering potential.

CHAPTER 6 CONCLUSION

Our study demonstrated that highly porous CS/BCP/TSA scaffolds could be constructed using a simple freeze-drying technique. The addition of BCP to the CS improved mechanical properties and delayed the degradation rate. Scaffolds with 20% of BCP and 800 nM of TSA showed excellent physicochemical structure, biocompatibility, and sustained release of TSA for up to 3 days. TSA released can inhibit histone deacetylase enzyme in hPDLs resulting in upregulating most osteoblast-related genes. The CS/BCP/TSA scaffolds' excellent bone regeneration capability was confirmed in the mice calvarial model. This study provided CS/BCP/TSA scaffolds as an up-and-coming candidate for bone tissue engineering applications.



APPENDIX



Appendix Figure 1. Mouse calvaria defect model. (A) A schematic illustration of animal experiments. (B) Surgical steps: calvaria shave and disinfect, defect created by biopsy punch, scaffold placement, and wound closure by suture.

REFERENCES

1. Fillingham Y, Jacobs J. Bone grafts and their substitutes. *The bone & joint journal*. 2016;98-B(1 Suppl A):6-9.
2. Florencio-Silva R, Sasso GR, Sasso-Cerri E, Simoes MJ, Cerri PS. Biology of Bone Tissue: Structure, Function, and Factors That Influence Bone Cells. *BioMed research international*. 2015;2015:421746.
3. Bouler JM, Pilet P, Gauthier O, Verron E. Biphasic calcium phosphate ceramics for bone reconstruction: A review of biological response. *Acta biomaterialia*. 2017;53:1-12.
4. Velasco MA, Narvaez-Tovar CA, Garzon-Alvarado DA. Design, materials, and mechanobiology of biodegradable scaffolds for bone tissue engineering. *BioMed research international*. 2015;2015:729076.
5. Amini AR, Laurencin CT, Nukavarapu SP. Bone tissue engineering: recent advances and challenges. *Critical reviews in biomedical engineering*. 2012;40(5):363-408.
6. Hutmacher DW. Scaffolds in tissue engineering bone and cartilage. *Biomaterials*. 2000;21(24):2529-43.
7. Liu Y, Lim J, Teoh SH. Review: development of clinically relevant scaffolds for vascularised bone tissue engineering. *Biotechnology advances*. 2013;31(5):688-705.
8. Bose S, Roy M, Bandyopadhyay A. Recent advances in bone tissue engineering scaffolds. *Trends in biotechnology*. 2012;30(10):546-54.
9. Dodane V, Vilivalam VD. Pharmaceutical applications of chitosan. *Pharm Sci Technolo Today*. 1998;1(6):246-53.
10. Dornish M, Kaplan D, Skaugrud O. Standards and guidelines for biopolymers in tissue-engineered medical products: ASTM alginate and chitosan standard guides. *American Society for Testing and Materials. Annals of the New York Academy of Sciences*. 2001;944:388-97.
11. Saravanan S, Leena RS, Selvamurugan N. Chitosan based biocomposite scaffolds for bone tissue engineering. *International journal of biological macromolecules*. 2016;93(Pt B):1354-65.

12. Saravanan S, Vimalraj S, Lakshmanan G, Jindal A, Sundaramurthi D, Bhattacharya J. Chitosan-Based Biocomposite Scaffolds and Hydrogels for Bone Tissue Regeneration. In: Choi AH, Ben-Nissan B, editors. *Marine-Derived Biomaterials for Tissue Engineering Applications*. Singapore: Springer Singapore; 2019. p. 413-42.
13. Costa-Pinto AR, Reis RL, Neves NM. Scaffolds based bone tissue engineering: the role of chitosan. *Tissue engineering Part B, Reviews*. 2011;17(5):331-47.
14. Croisier F, Jérôme C. Chitosan-based biomaterials for tissue engineering. *Eur Polym J*. 2013;49(4):780-92.
15. LogithKumar R, KeshavNarayan A, Dhivya S, Chawla A, Saravanan S, Selvamurugan N. A review of chitosan and its derivatives in bone tissue engineering. *Carbohydrate polymers*. 2016;151:172-88.
16. Bellich B, D'Agostino I, Semeraro S, Gamini A, Cesaro A. "The Good, the Bad and the Ugly" of Chitosans. *Marine drugs*. 2016;14(5).
17. Islam S, Bhuiyan MAR, Islam MN. Chitin and Chitosan: Structure, Properties and Applications in Biomedical Engineering. *J Polym Environ*. 2016:1-13.
18. Muzzarelli RA, El Mehtedi M, Bottegoni C, Aquili A, Gigante A. Genipin-Crosslinked Chitosan Gels and Scaffolds for Tissue Engineering and Regeneration of Cartilage and Bone. *Marine drugs*. 2015;13(12):7314-38.
19. Chen P-H, Kuo T-Y, Liu F-H, Hwang Y-H, Ho M-H, Wang D-M, et al. Use of Dicarboxylic Acids To Improve and Diversify the Material Properties of Porous Chitosan Membranes. *J Agric Food Chem*. 2008;56(19):9015-21.
20. Mitra T, Sailakshmi G, Gnanamani A, Mandal AB. Studies on Cross-linking of succinic acid with chitosan/collagen. *J Mater Res*. 2013;16:755-65.
21. Bodnár M, Hartmann JF, Borbély J. Nanoparticles from Chitosan. *Macromol Symp*. 2005;227(1):321-6.
22. Suwattanachai P, Pimkhaokham A, Chirachanchai S. Multi-functional carboxylic acids for chitosan scaffold. *International journal of biological macromolecules*. 2019;134:156-64.
23. Szymanska E, Winnicka K. Stability of chitosan-a challenge for pharmaceutical and biomedical applications. *Marine drugs*. 2015;13(4):1819-46.
24. Young Hoon K, Ho Cheol K, Sang Hun S, Hong Sung K, Kyu Cheon K, Shi Hyun L.

Original Article : Osteoconductive Effect of Chitosan/Hydroxyapatite Composite Matrix on Rat Skull Defect. *Tissue Eng Regen Med.* 2011;8(1):23-31.

25. Lee JS, Baek SD, Venkatesan J, Bhatnagar I, Chang HK, Kim HT, et al. In vivo study of chitosan-natural nano hydroxyapatite scaffolds for bone tissue regeneration. *International journal of biological macromolecules.* 2014;67:360-6.

26. Bose S, Tarafder S. Calcium phosphate ceramic systems in growth factor and drug delivery for bone tissue engineering: a review. *Acta biomaterialia.* 2012;8(4):1401-21.

27. Burg KJ, Porter S, Kellam JF. Biomaterial developments for bone tissue engineering. *Biomaterials.* 2000;21(23):2347-59.

28. Uetanabaro LC, Claudino M, Zancan R, Zielak JC, Garlet GP, de Araujo MR. Osteoconductivity of Biphasic Calcium Phosphate Ceramic Improves New Bone Formation: A Histologic, Histomorphometric, Gene Expression, and Microcomputed Tomography Study. *Int J Oral Maxillofac Implants.* 2020;35(1):70-8.

29. Duan R, van Dijk LA, Barbieri D, de Groot F, Yuan H, de Bruijn JD. Accelerated bone formation by biphasic calcium phosphate with a novel sub-micron surface topography. *European cells & materials.* 2019;37:60-73.

30. Schopper C, Ziya-Ghazvini F, Goriwoda W, Moser D, Wanschitz F, Spassova E, et al. HA/TCP compounding of a porous CaP biomaterial improves bone formation and scaffold degradation--a long-term histological study. *Journal of biomedical materials research Part B, Applied biomaterials.* 2005;74(1):458-67.

31. Chissov VI, Sviridova IK, Sergeeva NS, Frank GA, Kirsanova VA, Achmedova SA, et al. Study of in vivo biocompatibility and dynamics of replacement of rat shin defect with porous granulated bioceramic materials. *Bull Exp Biol Med.* 2008;146(1):139-43.

32. Wang L, Zhang B, Bao C, Habibovic P, Hu J, Zhang X. Ectopic osteoid and bone formation by three calcium-phosphate ceramics in rats, rabbits and dogs. *PLoS One.* 2014;9(9):e107044.

33. Al-Omar NA, Al-Qutub MN, Ramalingam S, Al-Kindi M, Nooh N, Ar-Regaie A, et al. Bone Regeneration Using Bone Morphogenetic Protein-2 and Biphasic Calcium Phosphate With and Without Collagen Membrane in Calvarial Standardized Defects: An In Vivo Microcomputed Tomographic Experiment in Rats. *Int J Periodontics Restorative*

Dent. 2016;36 Suppl:s161-70.

34. Lee GH, Makkar P, Paul K, Lee B. Incorporation of BMP-2 loaded collagen conjugated BCP granules in calcium phosphate cement based injectable bone substitutes for improved bone regeneration. *Materials science & engineering C, Materials for biological applications*. 2017;77:713-24.
35. Sendemir-Urkmez A, Jamison RD. The addition of biphasic calcium phosphate to porous chitosan scaffolds enhances bone tissue development in vitro. *Journal of biomedical materials research Part A*. 2007;81(3):624-33.
36. Padalhin AR, Lee BT. Hemostasis and Bone Regeneration Using Chitosan/Gelatin-BCP Bi-layer Composite Material. *ASAIO J*. 2019;65(6):620-7.
37. Dupont C, Armant DR, Brenner CA. Epigenetics: definition, mechanisms and clinical perspective. *Seminars in reproductive medicine*. 2009;27(5):351-7.
38. Rando OJ, Ahmad K. Rules and regulation in the primary structure of chromatin. *Current opinion in cell biology*. 2007;19(3):250-6.
39. Marks DL, Olson RL, Fernandez-Zapico ME. Epigenetic control of the tumor microenvironment. *Epigenomics*. 2016;8(12):1671-87.
40. Kucukali CI, Kurtuncu M, Coban A, Cebi M, Tuzun E. Epigenetics of multiple sclerosis: an updated review. *Neuromolecular medicine*. 2015;17(2):83-96.
41. van der Harst P, de Windt LJ, Chambers JC. Translational Perspective on Epigenetics in Cardiovascular Disease. *J Am Coll Cardiol*. 2017;70(5):590-606.
42. Tripathy MK, Abbas W, Herbein G. Epigenetic regulation of HIV-1 transcription. *Epigenomics*. 2011;3(4):487-502.
43. Lakshmaiah KC, Jacob LA, Aparna S, Lokanatha D, Saldanha SC. Epigenetic therapy of cancer with histone deacetylase inhibitors. *J Cancer Res Ther*. 2014;10(3):469-78.
44. Lawlor L, Yang XB. Harnessing the HDAC-histone deacetylase enzymes, inhibitors and how these can be utilised in tissue engineering. *International journal of oral science*. 2019;11(2):20.
45. Zhao Q, Ji K, Wang T, Li G, Lu W, Ji J. Effect of the Histone Deacetylases Inhibitors on the Differentiation of Stem Cells in Bone Damage Repairing and Regeneration. *Curr Stem Cell Res Ther*. 2020;15(1):24-31.

46. Hesham HM, Lasheen DS, Abouzid KAM. Chimeric HDAC inhibitors: Comprehensive review on the HDAC-based strategies developed to combat cancer. *Medicinal research reviews*. 2018;38(6):2058-109.
47. Huynh NC, Everts V, Pavasant P, Ampornaramveth RS. Inhibition of Histone Deacetylases Enhances the Osteogenic Differentiation of Human Periodontal Ligament Cells. *J Cell Biochem*. 2016;117(6):1384-95.
48. Huynh NC, Everts V, Nifuji A, Pavasant P, Ampornaramveth RS. Histone deacetylase inhibition enhances in-vivo bone regeneration induced by human periodontal ligament cells. *Bone*. 2017;95:76-84.
49. Huynh NC, Everts V, Ampornaramveth RS. Histone deacetylases and their roles in mineralized tissue regeneration. *Bone reports*. 2017;7:33-40.
50. Algate K, Haynes D, Fitzsimmons T, Romeo O, Wagner F, Holson E, et al. Histone deacetylases 1 and 2 inhibition suppresses cytokine production and osteoclast bone resorption in vitro. *J Cell Biochem*. 2020;121(1):244-58.
51. Nakamura T, Kukita T, Shobuike T, Nagata K, Wu Z, Ogawa K, et al. Inhibition of histone deacetylase suppresses osteoclastogenesis and bone destruction by inducing IFN-beta production. *J Immunol*. 2005;175(9):5809-16.
52. Zhang C, Wang X, Zhang E, Yang L, Yuan H, Tu W, et al. An epigenetic bioactive composite scaffold with well-aligned nanofibers for functional tendon tissue engineering. *Acta biomaterialia*. 2018;66:141-56.
53. Lee SU, Kwak HB, Pi SH, You HK, Byeon SR, Ying Y, et al. In Vitro and In Vivo Osteogenic Activity of Largazole. *ACS Med Chem Lett*. 2011;2(3):248-51.
54. Sukpaita T, Chirachanchai S, Suwattanachai P, Everts V, Pimkhaokham A, Ampornaramveth RS. In Vivo Bone Regeneration Induced by a Scaffold of Chitosan/Dicarboxylic Acid Seeded with Human Periodontal Ligament Cells. *International journal of molecular sciences*. 2019;20(19).
55. Murphy CM, Haugh MG, O'Brien FJ. The effect of mean pore size on cell attachment, proliferation and migration in collagen-glycosaminoglycan scaffolds for bone tissue engineering. *Biomaterials*. 2010;31(3):461-6.
56. Ghassemi T, Shahroodi A, Ebrahimzadeh MH, Mousavian A, Movaffagh J, Moradi A. Current Concepts in Scaffolding for Bone Tissue Engineering. *Arch Bone Jt Surg*.

2018;6(2):90-9.

57. Polo-Corrales L, Latorre-Esteves M, Ramirez-Vick JE. Scaffold design for bone regeneration. *J Nanosci Nanotechnol*. 2014;14(1):15-56.
58. Aslam Khan MU, Abd Razak SI, Al Arjan WS, Nazir S, Sahaya Anand TJ, Mehboob H, et al. Recent Advances in Biopolymeric Composite Materials for Tissue Engineering and Regenerative Medicines: A Review. *Molecules*. 2021;26(3).
59. Sareethammanuwat M, Boonyuen S, Arpornmaeklong P. Effects of beta-tricalcium phosphate nanoparticles on the properties of a thermosensitive chitosan/collagen hydrogel and controlled release of quercetin. *Journal of biomedical materials research Part A*. 2021;109(7):1147-59.
60. Dasgupta S, Maji K, Nandi SK. Investigating the mechanical, physiochemical and osteogenic properties in gelatin-chitosan-bioactive nanoceramic composite scaffolds for bone tissue regeneration: In vitro and in vivo. *Materials science & engineering C, Materials for biological applications*. 2019;94:713-28.
61. Cho YD, Kim WJ, Ryoo HM, Kim HG, Kim KH, Ku Y, et al. Current advances of epigenetics in periodontology from ENCODE project: a review and future perspectives. *Clin Epigenetics*. 2021;13(1):92.
62. Young DA, Barter MJ, Soul J. Osteoarthritis year in review: genetics, genomics, epigenetics. *Osteoarthritis Cartilage*. 2022;30(2):216-25.
63. Li Q, Liu F, Dang R, Feng C, Xiao R, Hua Y, et al. Epigenetic modifier trichostatin A enhanced osteogenic differentiation of mesenchymal stem cells by inhibiting NF-kappaB (p65) DNA binding and promoted periodontal repair in rats. *J Cell Physiol*. 2020;235(12):9691-701.
64. Zhang Y, Yu T, Peng L, Sun Q, Wei Y, Han B. Advancements in Hydrogel-Based Drug Sustained Release Systems for Bone Tissue Engineering. *Front Pharmacol*. 2020;11:622.
65. Huynh NC, Everts V, Akira N, Pavasant P, Ampornaramveth RS. Histone deacetylase inhibition enhances in-vivo bone regeneration induced by human periodontal ligament cells. *Bone*. 2016.



จุฬาลงกรณ์มหาวิทยาลัย
CHULALONGKORN UNIVERSITY



จุฬาลงกรณ์มหาวิทยาลัย
CHULALONGKORN UNIVERSITY

VITA

NAME	Teerawat Sukpaita
DATE OF BIRTH	15 Febuary 1989
PLACE OF BIRTH	Bangkok
HOME ADDRESS	222/97 Parkland Ratchada-thrapra



จุฬาลงกรณ์มหาวิทยาลัย
CHULALONGKORN UNIVERSITY